American Mineralogist, Volume 90, pages 639–644, 2005

Re-examination of the hydrogarnet structure at high pressure using neutron powder diffraction and infrared spectroscopy

GEORGE A. LAGER,[1,*] WILLIAM G. MARSHALL,[2] ZHENXIAN LIU,[3] AND ROBERT T. DOWNS[4]

[1]Department of Geography and Geosciences, University of Louisville, Louisville, Kentucky 40292, U.S.A.
[2]ISIS Facility, CLRC Rutherford Appleton Laboratory, Chilton, Didcot OX11 0QX, U.K.
[3]Geophysical Laboratory, Carnegie Institute of Washington, Washington, D.C. 20015, U.S.A.
[4]Department of Geosciences, University of Arizona, Tucson, Arizona 95721, U.S.A.

ABSTRACT

Time-of-flight neutron powder data and synchrotron infrared absorption spectra were collected for katoite hydrogarnet [$Ca_3Al_2(O_4D_4)_3$] at pressures to 9.4 and 9.8 GPa, respectively. The phase transition from space group $Ia3d$ to $I\bar{4}3d$ was observed in the neutron spectrum at ~7.5 GPa, as indicated by the presence of two weak reflections (730 and 530) that violate the hkl conditions ($hk0$, $h \neq 2n$) imposed by the a-glide operation. However, attempts to refine the high-pressure structure in space group $I\bar{4}3d$ did not significantly improve the fit and produced a chemically unreasonable O-D bond length at the second D position. Structure refinements in $Ia3d$ indicate that (1) the O-D bond length, corrected for the effects of thermal motion, remains essentially constant (~0.95 Å) with increasing pressure; (2) hydrogen bond lengths shorten with increasing pressure; however, the variation in O-D···O angles indicates a preferential strengthening of H bonds; and (3) the compression mechanism is characterized by bond shortening rather than bond bending. The new results are in excellent agreement with both high-pressure X-ray diffraction experiments and ab initio calculations, and illustrate the need to eliminate peak broadening in high-pressure neutron powder experiments. IR spectra collected for the same sample showed discontinuities in both O-H and O-D vibrational frequencies at ~5 GPa, suggesting that deuteration does not significantly affect the pressure of the transition. The higher pressure observed for the transition in the neutron data is probably due to lower signal-to-noise levels, which mask the weaker, symmetry-forbidden reflections at lower pressure.

INTRODUCTION

Katoite hydrogarnet [$Ca_3Al_2(O_4H_4)_3$] is a model for the incorporation of OH in garnets and other silicate minerals that occur in the mantle, e.g., coesite (Koch-Muller et al. 2003). In natural systems, Ca-silicate garnets may be important water-bearing phases in eclogitic regions of the upper mantle (O'Neill et al. 1993). Recent deformation experiments carried out at 3 GPa suggest that very small amounts of fluids released by garnets and pyroxenes in eclogites can migrate to grain boundaries where they induce melting and cause brittle failure (Zhang et al. 2002). For these reasons, there has been continued interest in the high-pressure crystal chemistry of katoite.

The first high-pressure structural study of katoite was carried out using neutron powder diffraction methods (Lager and Von Dreele 1996). In their experiment, the sample was mixed with both fluorinert (pressure-transmitting medium) and NaCl (pressure calibrant) and pre-pressed into a sphere, which was then inserted between the WC anvils in a Paris-Edinburgh cell. Significant peak broadening was observed in the spectra above 2–3 GPa due to non-hydrostatic conditions within the cell. The results of that neutron powder study have been shown to be inconsistent with both theoretical and experimental studies (Knittle et al. 1992; Nobes et al. 2000a, 2000b), suggesting that peak broadening plus overlap between garnet and NaCl peaks may have introduced systematic errors in the data above ~3 GPa. In the present study, the powder data were recollected from a fully deuterated katoite using a fluid pressure medium (deuterated ethanol:methanol). As the equation of state is well-determined (Lager et al. 2002), the sample was loaded without an internal pressure calibrant. In addition, the same sample was studied with high-pressure synchrotron IR spectroscopy to determine the effect of deuteration on the pressure of the phase transition.

EXPERIMENTAL METHODS

The polycrystalline samples of deuterated katoite (~1 g) were synthesized from tricalcium aluminate ($Ca_3Al_2O_6$) at 473 K in a Parr vessel (45 mL) filled to approximately 70% capacity with D_2O (99.9 at% D, Aldrich 15,188-2). The tricalcium aluminate was synthesized following the procedure described by Lager et al. (1987).

About 170 mg of powdered sample were loaded into a type V4b Paris-Edinburgh high-pressure cell (Besson et al. 1992) equipped with standard profile WC/Ni-binder anvils. The sample was confined between the anvils with a soft-metal-encapsulated (SME), single-toroid gasket machined from null-scattering Ti-Zr alloy (Marshall and Francis 2002). A standard 4:1 by volume mixture of deuterated methanol and ethanol was used as the pressure-transmitting medium. Oil pressure in the in situ ram was raised using a hand-operated hydraulic pump.

Time-of-flight (TOF) neutron powder diffraction data were collected at 0.08, 0.80, 1.72, 2.98, 4.05, 5.40, 6.65, 7.55, 8.56, and 9.42 GPa with the PEARL/HiPr diffractometer at the U.K. pulsed spallation source, ISIS. Integrated ISIS currents ranged from 560 μA·h (~3 h at 0.08 GPa) to 1883 μA·h (~11 h at 9.42 GPa). The equation of state determined by Lager et al. (2002) from single-crystal X-ray diffraction measurements was used to calculate the pressure (±0.1 GPa)

The overall d-spacing focused time-of-flight powder diffraction pattern obtained using the PEARL/HiPr 90° detector bank was corrected for neutron attenua-

* E-mail: galager@louisville.edu

tion by the anvil and gasket materials and normalized to the incident spectrum using a local routine. Although the WC anvils were shielded with cadmium foil, a small amount of contaminant Bragg scattering from the anvil materials was observed in all profiles. No significant pressure-induced peak broadening was observed with increasing pressure. The TOF peak profile was modeled with an exponential pseudo-Voigt function (function 3; Larson and Von Dreele 1994); the background with a standard 10-term cosine Fourier series (function 2; Larson and Von Dreele 1994). Two weak reflections of the type $hk0$ with $h \neq 2n$ were observed in the spectrum at 7.55 GPa. The presence of these reflections indicates loss of the *a*-glide plane and is consistent with the phase transition at ~5 GPa from $Ia3d$ to $I\bar{4}3d$ symmetry reported in a recent single-crystal X-ray study (Lager et al. 2002). By analogy with the X-ray study, the intensities of the symmetry-forbidden reflections in the neutron spectra should increase as the transition becomes fully developed above 5 GPa. It is likely that additional reflections are also present in the 5.40 GPa spectrum. However, they would be very weak in intensity and masked by the higher background levels typically associated with high-pressure neutron experiments.

In space group $I\bar{4}3d$, Ca and Al occupy positions [x, 0, 1/4] and [x, x, x], respectively. There are two non-equivalent O and H positions, i.e., two non-equivalent (O_4H_4) units. An attempt was made to refine the 9.4 GPa structure in space group $I\bar{4}3d$. The refinement was initiated with the X-ray positions for the non-D atoms. The D position refined by Lager et al. (1987) was used as a starting value for D1; the starting value for the D2 position was assumed to be near a D position which is symmetry equivalent to D1 in space group $Ia3d$ and within a radius of ~1 Å of O2. Refinement in $I\bar{4}3d$ did not significantly improve the fit and produced a chemically unreasonable O-D bond length at the D2 position. This is not surprising, given the subtle spectral changes that occur at the transition pressure. As a result, all structure refinements were carried out in space group $Ia3d$ (GSAS; Larson and Von Dreele 1994). Based on the refined D-site occupancy, the sample was fully deuterated. The final refinement profile at 9.42 GPa is shown in Figure 1. Atom positions, displacement parameters, hydrogen bond distances and angles, and other details relating to the refinement are given in Table 1. With the exception of the D atom, all atoms were refined with isotropic displacement parameters. The D atom exhibited a very anisotropic displacement ellipsoid with the maximum and minimum axes approximately perpendicular and parallel, respectively, to the direction of the O-D bond. This is consistent with results from previous neutron diffraction studies (e.g., Lager et al. 1987), and justified the inclusion of additional parameters in the refinement.

High-pressure synchrotron infrared (IR) measurements were performed at the U2A beamline at the National Synchrotron Light Source (NSLS), Brookhaven National Laboratory. The optical layout of the beamline facility has been described in detail elsewhere (Liu et al. 2002). The IR spectra were collected with a Bruker 66/S vacuum Fourier transform interferometer (FTIR) and Bruker IRscope-II microscope equipped with a HgCdTe type-A detector. The optical bench was evacuated and the microscope purged with dry nitrogen gas during the measurements to eliminate water vapor absorption. The resolution in the present study is 4 cm^{-1} with 1024 scans for all measurements.

High pressure was generated in a symmetric cell using a pair of type-II diamond anvils (500 μm culet). A ~100 μm-diameter hole was drilled in the center of a pre-indented steel gasket. To avoid any saturated absorption in the O-H stretching

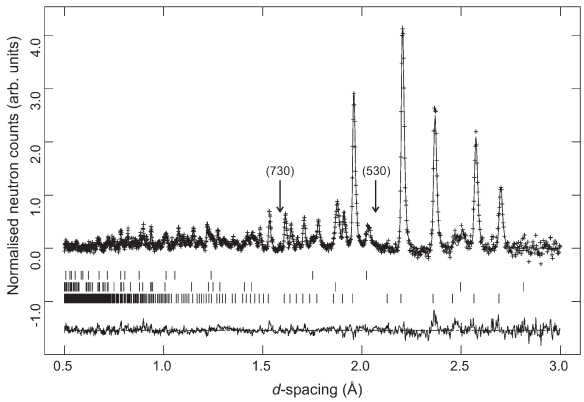

FIGURE 1. Final refinement profile for katoite at 9.42 GPa. Plus signs represent observed data. The solid line is the best-fit profile. Tick marks below the profile indicate the positions of the allowed reflections in each of the three phases: from bottom to top, katoite, WC, and Ni. The background was fit as part of the refinement but was subtracted before plotting. Two very weak reflections (730 and 530) that violate the *a*-glide operation in space group $Ia3d$ are indicated by arrows above

TABLE 1. Refinement conditions, unit-cell and atomic parameters and selected distances and angles involving the deuterium atom

P (GPa)	0.08	0.80	1.72	2.98	4.05	5.40	6.65	7.55	8.56	9.42
R_{wp}(%)	3.4	3.2	3.2	2.6	2.9	3.0	2.3	2.9	2.7	2.8
Number of Reflections	734	775	767	754	719	728	712	686	683	661
χ^2	1.31	1.44	1.45	1.96	1.38	1.57	2.23	1.54	1.64	2.04
a (Å)	12.5670(3)	12.5163(3)	12.4557(3)	12.3783(3)	12.3165(3)	12.2441(4)	12.1812(3)	12.1388(4)	12.0926(4)	12.0549(3)
V (Å^3)	1984.7(2)	1960.8(2)	1932.5(1)	1896.6(1)	1868.4(1)	1835.6(2)	1807.5(1)	1788.7(2)	1768.3(2)	1751.8(2)
U_{iso}(Ca)	0.017(2)	0.023(3)	0.026(2)	0.027(2)	0.027(2)	0.029(2)	0.029(2)	0.026(2)	0.029(3)	0.023(2)
U_{iso}(Al)	0.008(3)	0.009(2)	0.008(2)	0.011(2)	0.014(3)	0.011(3)	0.015(2)	0.011(3)	0.017(3)	0.020(3)
Ox	0.0287(4)	0.0290(4)	0.0294(5)	0.0296(3)	0.0299(4)	0.0301(4)	0.0311(4)	0.0314(4)	0.0312(5)	0.0316(4)
y	0.0521(4)	0.0519(4)	0.0523(4)	0.0517(3)	0.0521(4)	0.0534(4)	0.0522(3)	0.0515(4)	0.0525(4)	0.0525(4)
z	0.6421(3)	0.6420(4)	0.6421(3)	0.6419(3)	0.6426(3)	0.6423(3)	0.6437(3)	0.6445(4)	0.6432(4)	0.6439(3)
U_{iso}	0.018(2)	0.021(1)	0.023(1)	0.0184(7)	0.0181(9)	0.016(1)	0.021(1)	0.018(1)	0.018(1)	0.019(1)
Dx	0.1532(4)	0.1532(4)	0.1535(4)	0.1528(4)	0.1525(4)	0.1516(5)	0.1516(4)	0.1514(5)	0.1529(5)	0.1528(5)
y	0.0908(4)	0.0902(4)	0.0893(4)	0.0881(3)	0.0876(5)	0.0875(5)	0.0876(4)	0.0873(6)	0.0853(6)	0.0859(6)
z	0.7977(5)	0.7991(5)	0.7997(5)	0.8001(4)	0.8012(5)	0.8009(6)	0.8034(5)	0.8038(6)	0.8030(7)	0.8037(6)
U_{eq}	0.059	0.062	0.068	0.070	0.075	0.077	0.088	0.087	0.093	0.089
U_{11}	0.021(3)	0.025(3)	0.033(3)	0.036(3)	0.034(3)	0.041(4)	0.041(3)	0.039(4)	0.060(5)	0.059(4)
U_{22}	0.051(4)	0.058(4)	0.060(4)	0.067(3)	0.068(4)	0.069(5)	0.088(4)	0.090(6)	0.091(6)	0.102(6)
U_{33}	0.105(6)	0.102(5)	0.110(5)	0.107(4)	0.122(6)	0.124(7)	0.133(6)	0.132(7)	0.129(7)	0.107(5)
U_{12}	–0.004(3)	–0.008(2)	–0.013(3)	–0.020(2)	–0.023(3)	–0.030(3)	–0.035(3)	–0.035(3)	–0.046(4)	–0.054(4)
U_{13}	–0.015(3)	–0.021(3)	–0.017(3)	–0.020(2)	–0.022(3)	–0.023(4)	–0.024(3)	–0.023(4)	–0.037(4)	–0.041(4)
U_{23}	0.020(3)	0.020(3)	0.030(3)	0.033(3)	0.031(4)	0.030(4)	0.040(3)	0.050(4)	0.057(4)	0.069(4)
O-D	0.884(5)	0.878(5)	0.868(5)	0.872(4)	0.867(4)	0.873(5)	0.851(4)	0.845(5)	0.833(5)	0.828(5)
O-D*	0.95	0.95	0.94	0.96	0.96	0.97	0.96	0.96	0.96	0.95
D1···O3	2.551(9)	2.552(9)	2.541(10)	2.523(7)	2.507(8)	2.482(10)	2.449(8)	2.440(11)	2.446(11)	2.428(10)
D1···O3′	2.499(9)	2.475(9)	2.455(10)	2.416(8)	2.392(9)	2.382(10)	2.339(8)	2.314(10)	2.316(10)	2.306(9)
D3···O1′	2.606(9)	2.580(9)	2.560(9)	2.540(8)	2.513(9)	2.486(10)	2.475(8)	2.460(10)	2.461(9)	2.451(9)
O1-D1···O3	133.5(6)	131.9(6)	131.5(7)	130.4(5)	129.6(7)	130.5(8)	127.2(7)	126.3(8)	127.8(8)	127.2(8)
O1-D1···O3′	139.6(3)	141.0(5)	141.9(5)	143.3(4)	143.6(5)	142.5(6)	143.5(5)	143.8(6)	146.0(6)	145.4(6)
O3-D3···O1′	111.1(7)	112.2(7)	112.0(7)	112.3(6)	112.7(7)	111.0(9)	114.6(7)	115.6(9)	112.9(9)	113.9(9)
D1···D3′	1.956(9)	1.950(9)	1.935(10)	1.903(8)	1.893(10)	1.870(11)	1.882(9)	1.873(12)	1.845(12)	1.853(12)
D3···D1′	2.063(11)	2.038(12)	2.033(13)	2.017(11)	1.991(13)	1.971(15)	1.921(13)	1.909(17)	1.960(17)	1.935(16)

* Bond length corrected for the effects of thermal motion using a simple riding model of the form $R^2_{SRB}(OD) = R^2(OD) + 3[U_{iso}(D) - U_{iso}(O)]$ (Downs et al. 1992).

vibrational region, a thin film (<1 mμ in thickness) was made by compressing a small amount of powder between the diamond anvils. The film was ~50 μm in diameter and slightly off-center of the gasket hole. The KBr powder and a few ruby chips were loaded into the gasket hole as pressure medium and pressure gauge, respectively (Mao et al. 1986). The upper aperture was set at 30×30 μm^2.

Results and discussion

Comparison of neutron powder results with previous studies

The general formula of hydrogarnet can be represented as $^{[8]}X_3{}^{[6]}Y_2(^{[4]}SiO_4)_{3-x}(O_4H_4)_x$, where the superscripts in brackets refer to the O coordination of the three types of cations in the structure. The coordination of the X site by oxygen can be defined as a triangular dodecahedron (distorted cube) that shares two edges with tetrahedra, four with octahedra (Y site) and four with other dodecahedra. The dodecahedral cavities are located within a framework composed of corner-sharing octahedra and tetrahedra (Novak and Gibbs 1971). When Si does not occupy the tetrahedron, each O atom surrounding the vacancy is bonded to H. In space group *Ia*3*d*, the hydrogarnet structure is uniquely defined by the fractional coordinates of O and H atoms and by the unit-cell parameter. The cation positions are fixed by symmetry.

Akhmatskaya et al. (1999) defined four parameters to illustrate the affect of pressure on polyhedral distortion: bond-length distortion of the dodecahedron, the edge-length distortion of the octahedron, and the angular distortion of the octahedron and tetrahedron. Figure 2 shows how the distortion parameters obtained in the present study compare with those from theoretical calculations (Nobes et al. 2000a, 2000b), high-pressure single-crystal X-ray refinements (Lager et al. 2002), and previous neutron powder diffraction refinements (Lager and Von Dreele 1996) (Fig. 2). In contrast to the three more recent studies, distortion parameters calculated from the data of Lager and Von Dreele (1996) show a nonlinear behavior above ~3 GPa. If fluorinert is used as the pressure-transmitting medium, it is well known that deviatoric stress in the sample environment can cause strain broadening of Bragg reflections and loss of resolution above this pressure. The loss of resolution coupled with the overlap of sample and pressure standard peaks may have introduced systematic errors in the data. On the other hand, agreement between the new neutron powder data and theoretical and X-ray studies is excellent, suggesting, at least in this case, that the elimination of strain broadening is essential to the correct interpretation of high-pressure neutron powder data.

Lager and Von Dreele (1996) concluded that the compression mechanism in katoite is characterized by a cooperative rotation of corner-sharing tetrahedra and octahedra, similar to that observed in andradite (Hazen and Finger 1989). The new powder data are consistent with both theoretical and X-ray studies, which showed that compression is dominated by bond shortening rather than bond bending.

Phase transition at 5 GPa

The single-crystal X-ray study carried out by Lager et al. (2002) revealed that katoite undergoes a phase transition from *Ia*3*d* to $I\bar{4}3d$ at ~5 GPa. The transition was recognized by the presence of several weak reflections of the type *hk*0 with $h \neq 2n$, indicating loss of the *a*-glide plane. Based on the analysis of the hydrogarnet structure, it was proposed that compression of the short D-D distance between (O_4D_4) tetrahedra might destabilize the structure and initiate the transition. To corroborate this model, accurate information on the pressure dependence of the hydrogen atom positions is required. Therefore, one objective of the present study was to determine if the transition could be observed by neutron diffraction. As noted previously, the transition is also detected in the neutron data but it appears to occur at a higher pressure (>6.65 GPa) than found in the X-ray experiment.

To determine if deuteration affected the pressure of the tran-

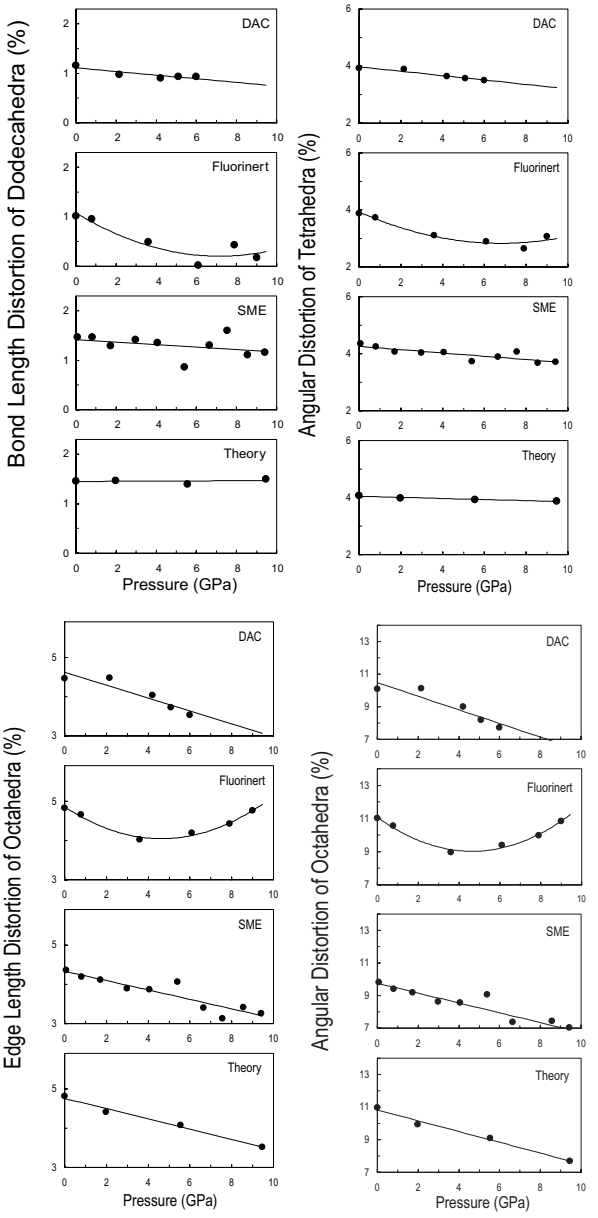

Figure 2. Distortion parameters, as defined by Akhmatskaya et al. (1999), plotted as a function of pressure for four high-pressure katoite studies: single-crystal X-ray refinements (DAC), Lager et al. (2002); neutron powder refinements (fluorinert), Lager and Von Dreele (1996); present study (SME); theoretical calculations (theory), Nobes et al. (2000a, 2000b).

sition, high-pressure IR spectra (Fig. 3) were collected for the same sample to 9.81 GPa using KBr as the pressure-transmitting medium. Inspection of the O-H stretching region at ambient pressure revealed that significant H → D exchange had occurred in the sample subsequent to the neutron experiment, probably during unloading of the Paris-Edinburgh cell. The frequencies of both the O-D and O-H bands show a slight decrease from ambient pressure to ~5 GPa, which is consistent with strengthening of hydrogen bonding with increasing pressure (see below). Above 5 GPa, there is an obvious discontinuity in both O-H and O-D frequencies that corresponds to the phase transition from *Ia*3*d* to $I\bar{4}3d$. Assuming a small isotopic effect with increasing H/D ratio, i.e., the pressure dependence of the O-D frequency is similar for a fully deuterated katoite, one can conclude that deuteration has little or no effect on the pressure of the transition.

In the $I\bar{4}3d$ structure, there are two unique oxygen atoms and two OH groups. The peak broadening in the IR spectra above ~5 GPa may be due to an additional band associated with the second O-D(H) group; however, this is difficult to determine because the broadening is also related to the use of KBr as the pressure-transmitting medium.

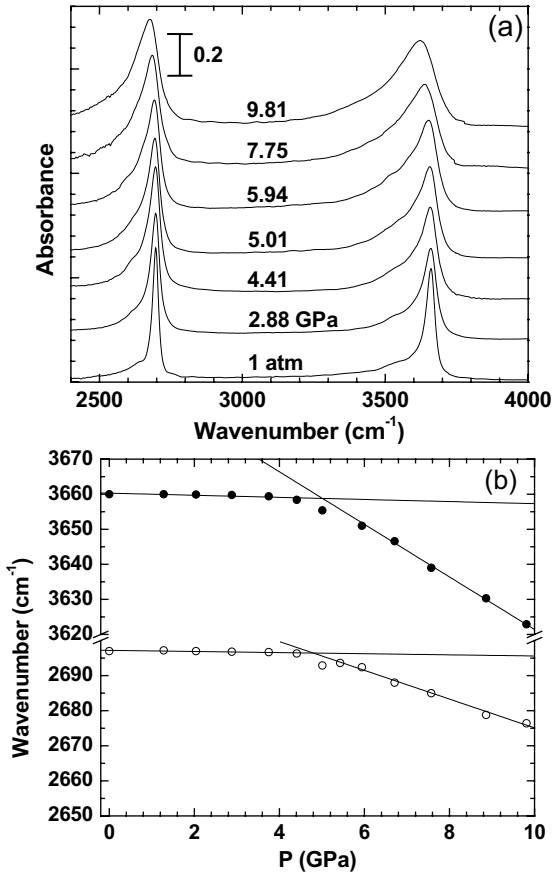

FIGURE 3. Synchrotron IR data showing (**a**) the O-H and O-D stretching bands as a function of pressure and (**b**) the discontinuity in the O-H and O-D frequencies at ~5 GPa.

Hydrogen atom environment at high pressure

The hydrogen atom environment in the katoite structure is illustrated in Figure 4. The variation in the O-D bond length at high pressure is compared with theoretical values and those determined in the previous neutron powder study of Lager and Von Dreele (1996) in Figure 5. The pressure dependence of hydrogen bond distances and angles and D···D distances are plotted

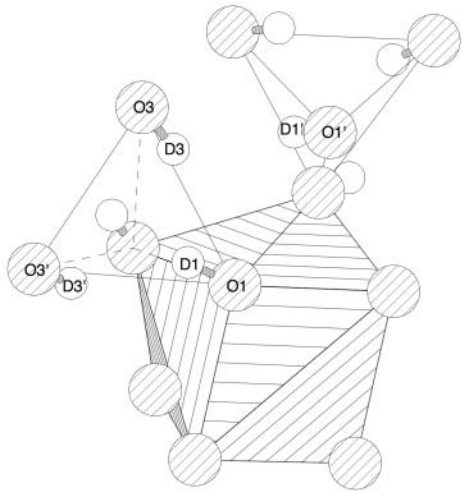

FIGURE 4. Structure drawing of adjacent O_4D_4 tetrahedra and CaO_8 dodecahedron in katoite at 0.08 GPa. Three H bonds with lengths <2.60 Å are formed at ambient pressure: D1···O3, D1···O3', and D3···O1'.

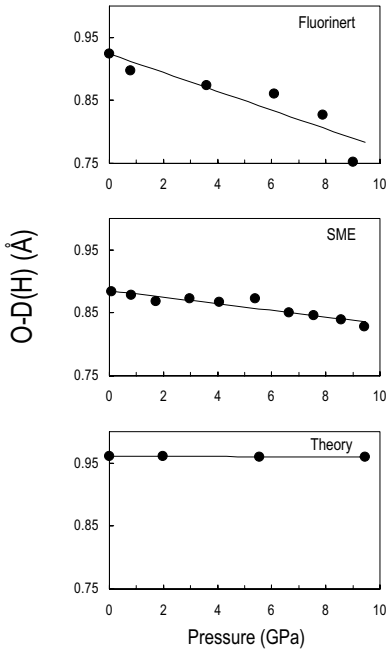

FIGURE 5. Variation in the O-D(H) bond length as a function of pressure: powder neutron diffraction study (fluorinert), Lager and Von Dreele (1996); present study (SME); theoretical calculation (theory), Nobes et al. (2000a, 2000b). The estimated standard deviations are approximately equal to the size of the symbols in this and subsequent figures.

together with theoretical values in Figures 6–8. With the exception of the O-H bond distance, there is good agreement between the new experimental data and ab initio calculations based on density functional theory (Nobes et al. 2000a, 2000b). Figure 5 shows that the O-D bond is significantly shorter than the average O-H distance (~0.96 Å) determined by neutron diffraction (Ceccarelli et al. 1981). However, as discussed by Lager et al. (2002), if this bond length is corrected for the effects of thermal motion, the experimental value is in good agreement with the calculated bond length.

At high pressure the uncorrected O-D bond exhibits an apparent shortening due to an increase in the D displacement amplitude perpendicular to the bond (Fig. 5). This change is reflected in the magnitudes of equivalent isotropic displacement factors (U_{eq}), which increase from 0.059 Å^2 at 0.08 GPa to 0.089 Å^2 at 9.42 GPa (Table 1). Application of a simple riding model results in a nearly constant O-D bond length (~0.95 Å) over the entire pressure range (Downs et al. 1992; Table 1), consistent with other recent neutron powder studies (e.g., Nelmes et al. 1993; Parise et al. 1994). The greater rate of decrease in the uncorrected O-D bond length observed by Lager and Von Dreele (1996) is probably related to systematic errors in the data, as discussed above (Fig. 5). Nevertheless, if the riding model correction is applied to these data, the resulting O-D bond length (~0.94 Å) is more consistent with experimental values and remains constant at pressures to 6.1 GPa (Lager et al. 2002). Although the riding model correction yields reasonable bond lengths in both neutron powder studies, it is not clear why the thermal motion of the D atom should increase at pressure. A similar effect could be produced by a pressure-dependent positional disorder.

Within the (O_4D_4) tetrahedron, the D1 atom forms a bifurcated hydrogen bond with O3 and O3'. If one considers all D atoms within a radius of 2.60 Å of an oxygen atom, an inter-tetrahedral H bond is also formed between D3 and O1' (Fig. 4). All three H bonds decrease linearly with increasing pressure, as predicted by theoretical calculations (Fig. 6). Higher pressures should favor the development of stronger H bonding for D1···O3' and D3···O1' as their associated O-D···O angles become larger (Fig. 7). In contrast to the theoretical study, the D-D distance between tetrahedra (D3···D1') decreases at about the same rate as the shortest D-D distance within the tetrahedron (D1···D3') (see Fig.

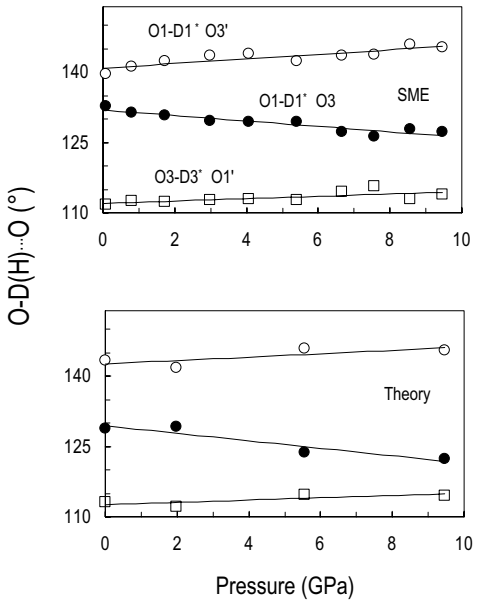

Figure 7. Variation in the O-D(H)···O bond angles as a function of pressure: present study (SME); theoretical calculation (theory), Nobes et al. (2000a, 2000b).

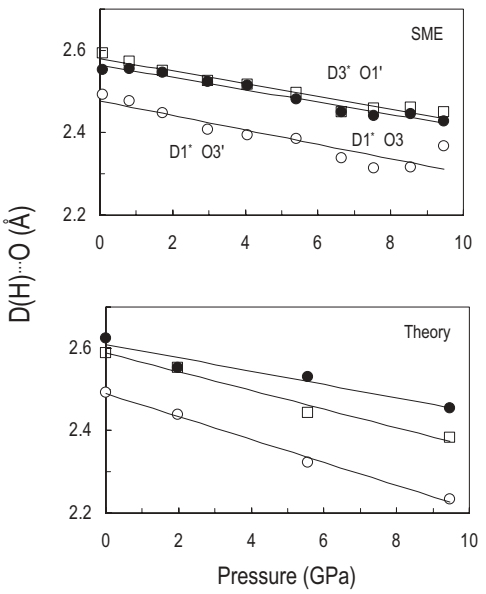

Figure 6. Variation in the D(H)···O bond length as a function of pressure: present study (SME); theoretical calculation (theory), Nobes et al. (2000a, 2000b).

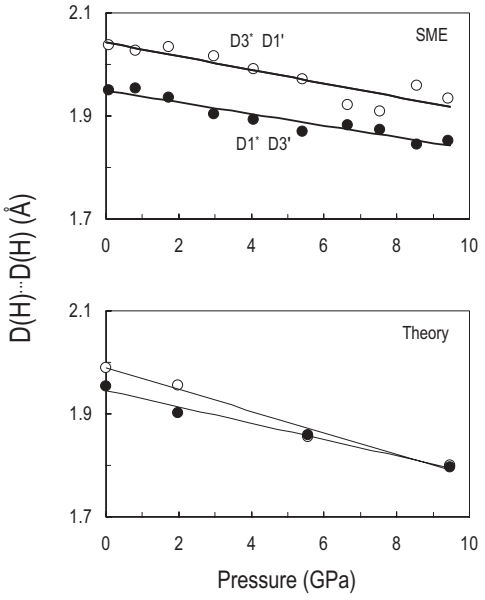

Figure 8. Variation in the D(H)···D(H) distances as a function of pressure: present study (SME); theoretical calculation (theory), Nobes et al. (2000a, 2000b).

4 and Fig. 8). As noted above, Lager et al. (2002) proposed that D-D repulsion due to the compression of the inter-tetrahedral D-D distance might initiate the transition to $I\bar{4}3d$. Unfortunately, the new data on the pressure dependence of the D···D distances offers no explanation as to the role of D···D interactions in the phase transition.

Pascale et al. (2004) have recently modeled the pressure dependence of the katoite structure using a localized, Gaussian-type basis set and hybrid B3-LYP Hamiltonians (Program CRYSTAL). These higher-level calculations predict a similar rate of compression for both the inter- and intra-tetrahedral H···H distances, in agreement with the experimental results shown in Fig. 8. In this case, the crossover point is at ~15 GPa rather than ~8 GPa, as predicted by density functional theory. However, neither calculation can predict the occurrence of the phase transition at ~5 GPa.

ACKNOWLEDGMENTS

G.A.L. acknowledges support from the National Science Foundation through grant EAR-0073734. We thank the ISIS Neutron Facility, CLRC Rutherford Appleton Laboratory for neutron beamtime, materials and other resources, and D.J. Francis for technical support on PEARL/HiPr. The authors thank M. Welch and S. Redfern for their constructive reviews.

REFERENCES CITED

Akhmatskaya, E., Nobes, R., Milman, V., and Winkler, B. (1999) Structural properties of garnets under pressure: an ab initio study. Zeitschrift fur Kristallographie, 214, 808–819.

Besson, J.M., Nelmes, R.J., Hamel, G., Loveday, J.S., Weill, G., and Hull, S. (1992) Neutron powder diffraction above 10 GPa. Physica B, 180–181, 907–910.

Ceccarelli, C., Jeffrey, G.A., and Taylor, R. (1981) A survey of O-H···O hydrogen bond geometries determined by neutron diffraction. Journal of Molecular Structure, 70, 255–271.

Downs, R.T., Gibbs, G.V., Bartelmehs, K.L., and Boisen, M.B., Jr. (1992) Variations of bond lengths and volumes of silicate tetrahedra with temperature. American Mineralogist, 77, 751–757.

Hazen, R.M. and Finger, L.W. (1989) High-pressure crystal chemistry of andradite and pyrope: Revised procedures for high-pressure diffraction experiments. American Mineralogist, 74, 352–59.

Knittle, E., Hathorne, A., Davis, M., and Williams, Q. (1992) A spectroscopic study of the high-pressure behavior of the O_4H_4 substitution in garnet. In Y. Syono and M.H. Manghnani, Eds., High-pressure research: Application to earth and planetary sciences, 67, 297–304. Geophysical Monograph, American Geophysical Union.

Koch-Müller, M., Dera, P., Fei, Y., Reno, B., Sobolev, N., Hauri, E., and Wysoczanski, R. (2003) OH^- in synthetic and natural coesite. American Mineralogist, 88, 1436–1445.

Lager, G.A. and Von Dreele, R.B. (1996) Neutron powder diffraction study of hydrogarnet to 9.0 GPa. American Mineralogist, 81, 1097–1104.

Lager, G.A., Armbruster, T., and Faber, J. (1987) Neutron and X-ray diffraction study of hydrogarnet $Ca_3Al_2(O_4H_4)_3$. American Mineralogist, 72, 756–765.

Lager, G.A., Downs, R.T., Origlieri, M., and Garoutte, R. (2002) High-pressure single-crystal X-ray diffraction study of katoite hydrogarnet: Evidence for a phase transition from $Ia3d$ to $I\bar{4}3d$ symmetry at 5 GPa. American Mineralogist, 87, 642–647.

Larson, A.C. and Von Dreele, R.B. (1994) General structure analysis system (GSAS). Los Alamos National Laboratory Report LAUR 96–748.

Liu, Z., Hu, J., Yang, H., Mao, H.K., and Hemley, R.J. (2002) High-pressure synchrotron X-ray diffraction and infrared microspectroscopy: applications to dense hydrous phases. Journal of Physics: Condensed Matter, 14, 10641–10646.

Mao, H.K., Xu, J., and Bell, P.M. (1986) Calibration of the ruby pressure gauge to 800 Kbar under quasi-hydrostatic conditions. Journal Geophysical Research, 91, 4673–4676.

Marshall, W.G. and Francis, D.J. (2002) Attainment of near-hydrostatic compression using the Paris-Edinburgh cell. Journal of Applied Crystallography, 35, 122–125.

Nelmes, R.J., Loveday, J.S., Wilson, R.M., Besson, J.M., Pruzan, P., Klotz, S., and Hull, S. (1993) Neutron diffraction study of deuterated ice VIII to 10 GPa. Physical Review Letters, 71, 1192–1195.

Nobes, R., Akhmatskaya, E., Milman, V., White, J., Winkler, B., and Pickard, C. (2000a) An ab initio study of hydrogarnets. American Mineralogist, 85, 1706–1715.

Nobes, R.H., Akhmatskya, E.V., Milman, V., Winkler, B., and Pickard, C.J. (2000b) Structure and properties of aluminosilicate garnets and katoite: an ab initio study. Computational Materials Science, 17, 141–145.

Novak, G.A. and Gibbs, G.V. (1971) Crystal chemistry of the silicate garnets. American Mineralogist, 56, 791–825.

O'Neill, B., Bass, J.D., and Rossman, G.R. (1993) Elastic properties of hydrogrossular garnet and implications for water in the upper mantle. Journal of Geophysical Research, 98(B11), 20,031–20,037.

Parise, J.B., Leinenweber, K., Weidner, D.J., Tan, K., and Von Dreele, R.B. (1994) Pressure-induced H bonding: Neutron diffraction study of brucite, $Mg(OH)_2$, to 9.3 GPa. American Mineralogist, 79, 193–196.

Pascale, F., Ugliengo, P., Civalleri, B., Orlando, R., D'Arco, P., and Dovesi, R. (2004) The katoite hydrogarnet Si-free $Ca_3Al_2([OH]_4)_3$: A periodic Hartree-Fock and B3-LYP study. Journal of Chemical Physics, 121, 1005–1013.

Zhang, J., Green, H.W., Bozhilov, K.N., and Zhenmin, J. (2002) Dehydration induced faulting in eclogite at high pressure: A mechanism for intermediate-focus earthquakes. EOS Transactions of the American Geophysical Union, 83(47).

MANUSCRIPT RECEIVED FEBRUARY 23, 2004
MANUSCRIPT ACCEPTED AUGUST 31, 2004
MANUSCRIPT HANDLED BY ALISON PAWLEY